Int. J. Solids Structures Vol. 30, No. 16, pp. 2261–2276, 1993
Printed in Great Britain

0020–7683/93 \$6.00+ .00

A FINITE ELEMENT ALTERNATING APPROACH TO THE BENDING OF THIN PLATES CONTAINING MIXED MODE CRACKS

WEN-HWA CHEN and CHIH-MING SHEN
Department of Power Mechanical Engineering, College of Engineering, National Tsing Hua University, Hsinchu, Taiwan 30043, Republic of China

(*Received* 21 *July* 1992 ; *in revised form* 28 *February* 1993)

Abstract—A finite element alternating procedure developed to deal with the cracked plate in symmetric bending is extended to analyse the more realistic case with single or multiple mixed mode cracks. This modified procedure involves the new derivation of the analytical solution for an infinite thin plate containing a crack subjected to arbitrary anti-symmetric equivalent shear force on crack surfaces. Due to the natural limitation of Kirchhoff assumptions for a thin plate in bending, the appropriate treatment of constant twisting moments on the crack surfaces is devised. The interaction effect among cracks on the calculation of bending (symmetric) and shear (anti-symmetric) stress intensity factors is also discussed. Several numerical examples are solved to demonstrate the validity and efficiency of the approach.

1. INTRODUCTION

The evaluation of the safety and strength remaining in a bending plate containing through cracks is of great importance in practical engineering applications. For such problems, Williams (1961) obtained the stress distribution in the vicinity of the crack-tip. Sih *et al.* (1962) used Williams' results to define bending (symmetric) and shear (anti-symmetric) stress intensity factors K_b and K_s. Because of the mathematical complexities involved in the analytical evaluation of K_b and K_s, only a small number of solutions for the problems with simple geometries and boundary conditions are available (Sih, 1973a).

To compute K_b and K_s for more realistic engineering problems, suitable numerical techniques are necessary. In the literature, to account for the singularity of the stress field near the crack-tip, various types of finite element models are developed (Barsoum, 1976 ; Yagawa and Nishioka, 1979 ; Ahmad and Loo, 1979 ; Rhee and Atluri, 1982 ; Chen and Chen, 1984 ; Ye and Gallagher, 1984 ; Murthy *et al.*, 1981). Among these surveys, the accuracy of the stress intensity factors obtained largely depends on either the mesh size selected or analysis model established. Further, as the problem with multiple cracks is solved, expensive computer time is consumed. To compensate for these shortcomings, an efficient technique that combines the advantages of finite element method and Schwarz's alternating method (Sih, 1973b) is then established. However, the so-called finite element alternating method has been successfully developed to solve the thin plate in bending with bending (symmetric) mode cracks only (Chen *et al.*, 1992). Thus, the aim of this work is to extend such methods to the analysis of the thin cracked plate in bending with single or multiple mixed mode (bending/shear) cracks. The present idea is similar in spirit to the procedures for singularity calculation within the so-called Hybrid–Trefftz finite element formulation (Jirousek, 1985 ; Jirousek and Guex, 1986 ; Jirousek and Venkatesh, 1990) and the auxiliary mapping technique (Babuška and Oh, 1990).

The present method involves the iterative superposition of the finite element solution of a bounded uncracked plate in bending and the analytical solution for an infinite thin plate containing a crack subjected to arbitrary symmetric bending moment (Chen *et al.*, 1992) and anti-symmetric equivalent shear force on crack surfaces. The bending moment and equivalent shear force evaluated at the location of fictitious cracks are fitted by appropriate polynomials through the least square method. In fact, the residual stresses at the location of fictitious cracks are due to bending, twisting moment and transverse shear force. But those three types of loadings cannot be applied to the crack surfaces directly. Kirchhoff assumptions show that the equivalent shear force can be expressed in terms of the derivative of twisting moment and transverse shear force (Szilard, 1974). Hence, based on the Kirchhoff assumptions for thin plate in bending, the constant twisting moment behaves as trivial in the computation of the equivalent shear force. Therefore, suitable treatment of the constant twisting moment is essential to compute accurate mixed mode (bending/shear) stress intensity factors.

In the present approach, the finite element mesh adopted is independent of the number, location, orientation and length of the cracks. Besides, because of the fast convergence of the solution, the computer time consumed is very economical as compared with those required by conventional finite element calculation especially for the case with multiple cracks.

To demonstrate the applicability and versatility of the present technique, several numerical examples are analysed. The interaction effect among cracks on the computation of bending and shear stress intensity factors is also studied in detail.

2. ANALYTICAL SOLUTION FOR A CRACK SUBJECTED TO ARBITRARY ANTI-SYMMETRIC EQUIVALENT SHEAR FORCE

To establish the finite element alternating procedure, an analytical solution of an infinite thin plate subjected to arbitrary symmetric bending moment and anti-symmetric equivalent shear force on crack surfaces is required. The former case has been solved by the principal author (Chen *et al.*, 1992). For completeness, the analytical solution of an infinite plate subjected to arbitrary anti-symmetric equivalent shear force needs to be derived here.

Based on classical plate theory (Szilard, 1974), in the absence of distributed lateral loading, the governing equation for a thin plate can be written as:

$$w_{,xxxx}+2w_{,xxyy}+w_{,yyyy} = 0. \tag{1}$$

The relations among the lateral deflection w and related variables are

$$m_x = -D(w_{,xx}+\nu w_{,yy}), \tag{2}$$

$$m_y = -D(w_{,yy}+\nu w_{,xx}), \tag{3}$$

$$m_{xy} = -D(1-\nu)w_{,xy}, \tag{4}$$

$$q_x = -D(w_{,xxx}+w_{,xyy}), \tag{5}$$

$$q_y = -D(w_{,xxy}+w_{,yyy}), \tag{6}$$

$$v_x = q_x+m_{xy,y} = -D[w_{,xxx}+(2-\nu)w_{,xyy}] \tag{7}$$

and

$$v_y = q_y+m_{yx,x} = -D[w_{,yyy}+(2-\nu)w_{,xxy}], \tag{8}$$

(m_x, m_y, m_{xy}), (q_x, q_y) and (v_x, v_y) represent the bending and twisting moments, transverse shear forces and equivalent shear forces per unit length of the plate. $D = Eh^3/12(1-\nu^2)$ is the flexural rigidity of the plate. E, h and ν denote Young's modulus, plate thickness and Poisson's ratio respectively.

To solve eqn (1), one can transform the variables (w, y) into the variables $(\hat{w}, \xi)$ by the Fourier transform technique (Sneddon, 1951) as:

$$\hat{w}(x, \xi) = \int_{-\infty}^{\infty} w(x, y)\, e^{i\xi y}\, dy,$$

where $i = \sqrt{-1}$ and the variable x has not been transformed. Then, eqns (1)–(8) become

$$\left(\frac{d^2}{dx^2} - \xi^2\right)^2 \hat{w}(x, \xi) = 0, \tag{9}$$

$$\hat{m}_x = -D(\hat{w}_{,xx} - v\xi^2 \hat{w}), \tag{10}$$

$$\hat{m}_y = -D(v\hat{w}_{,xx} - \xi^2 \hat{w}), \tag{11}$$

$$\hat{m}_{xy} = i(1-v)D\xi \hat{w}_{,x}, \tag{12}$$

$$\hat{q}_x = -D(w_{,xxx} - \xi^2 \hat{w}_{,x}), \tag{13}$$

$$\hat{q}_y = iD\xi(\hat{w}_{,xx} - \xi^2 \hat{w}), \tag{14}$$

$$\hat{v}_x = -D(w_{,xxx} - (2-v)\xi^2 \hat{w}_{,x}) \tag{15}$$

and

$$\hat{v}_y = iD\xi((2-v)\hat{w}_{,xx} - \xi^2 \hat{w}). \tag{16}$$

The solution of eqn (9) is thus obtained as follows:

$$\hat{w}(x, \xi) = (c_1 + c_2 x)\, e^{-|\xi| x} + (c_3 + c_4 x)\, e^{|\xi| x}, \tag{17}$$

where the coefficients c_1, c_2, c_3 and c_4 are functions of the variable ξ and can be determined by the given boundary conditions. The transformed $\hat{w}$ and $(\hat{m}_x, \hat{m}_y, \hat{m}_{xy}, \hat{q}_x, \hat{q}_y, \hat{v}_x, \hat{v}_y)$ are hence determined from eqns (10)–(17). After taking the inverse Fourier transform for these variables, one obtains the complete analytical solutions consistent with the thin plate theory. As seen in Fig. 1, based on the principle of superposition, the complete analytical solutions can be combined by those solutions of which crack surfaces are subjected to arbitrary symmetric bending moment [Fig. 1(b)] and arbitrary anti-symmetric equivalent shear force [Fig. 1(c)], respectively. Since the case as shown by Fig. 1(b) has been solved (Chen *et al.*, 1992), the attention is focused on solving the case of Fig. 1(c). To do this, as seen in

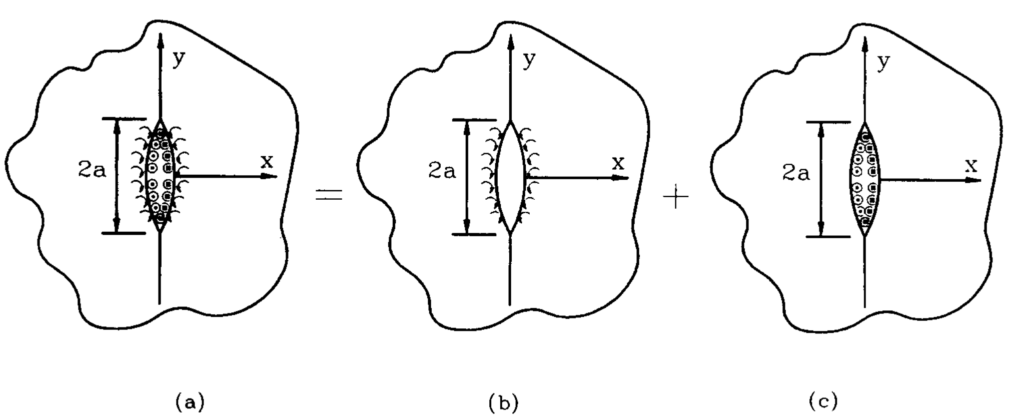

Fig. 1. An infinite thin plate containing a crack subjected to arbitrary symmetric bending moment and anti-symmetric equivalent shear force.

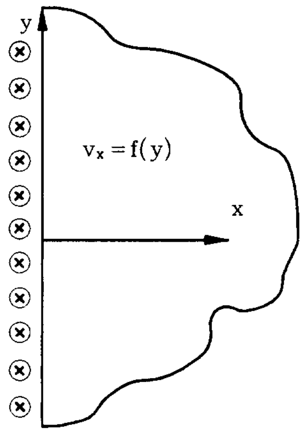

Fig. 2. A semi-infinite plate subjected to arbitrary equivalent shear force.

Fig. 2, the problem of a semi-infinite plate subjected to arbitrary equivalent shear force at one side needs to be analysed first. The boundary conditions for this problem can be listed as below:

(i) $v_x = f(y)$ at $x = 0$,

(from the equilibrium condition, $\int_{-\infty}^{\infty} v_x \, dy = 0$ is satisfied automatically),

(ii) $m_x = 0$ at $x = 0$

and

(iii) $w \to 0$ as $x \to \infty$.

By condition (iii), the constants c_3 and c_4 in eqn (17) must vanish. Thus, eqn (17) can be simplified to:

$$\hat{w}(x, \xi) = (c_1 + c_2 x)\, e^{-|\xi| x}. \tag{18}$$

Carrying out the Fourier transform on both sides of conditions (i) and (ii), we obtain

$$\hat{v}_x = \hat{f}(\xi) \tag{19}$$

and

$$\hat{m}_x = 0, \tag{20}$$

where $\hat{f}(\xi) = \int_{-\infty}^{\infty} f(y)\, e^{i\xi y}\, dy$. Substituting eqn (18) into eqns (10) and (15) and comparing with the variables $\hat{m}_x$ and $\hat{v}_x$ obtained by eqns (19) and (20), the constants c_1 and c_2 are determined and the transformed $\hat{w}(x, \xi)$ in eqn (18) can be thus found as:

$$\hat{w}(x, \xi) = \frac{-1}{(3+\nu)(1-\nu)D|\xi|^3} \hat{f}(\xi)(2 + (1-\nu)|\xi| x)\, e^{-|\xi| x}. \tag{21}$$

Now, substituting eqn (21) into eqns (10)–(16) and taking the inverse Fourier transform, respectively, the analytical solution of the semi-infinite thin plate is derived as:

$$w(x, y) = \frac{-1}{2\pi(3+\nu)(1+\nu)D} \int_{-\infty}^{\infty} \frac{\hat{f}(\xi)}{|\xi|^3} (2 + (1-\nu)|\xi| x)\, e^{-|\xi| x - i\xi y}\, d\xi, \tag{22}$$

$$m_x(x, y) = \frac{(1-\nu)x}{2\pi(3+\nu)} \int_{-\infty}^{\infty} \hat{f}(\xi)\, e^{-|\xi| x - i\xi y}\, d\xi, \tag{23}$$

$$m_y(x,y) = \frac{-1}{2\pi(3+\nu)} \int_{-\infty}^{\infty} \frac{\hat{f}(\xi)}{|\xi|} (2(1+\nu)+(1-\nu)|\xi|x)\, \mathrm{e}^{-|\xi|x-\mathrm{i}\xi y}\, \mathrm{d}\xi, \tag{24}$$

$$m_{xy}(x,y) = \frac{\mathrm{i}}{2\pi(3+\nu)} \int_{-\infty}^{\infty} \frac{\hat{f}(\xi)}{|\xi|^2}\, \xi((1+\nu)+(1-\nu)|\xi|x)\, \mathrm{e}^{-|\xi|x-\mathrm{i}\xi y}\, \mathrm{d}\xi, \tag{25}$$

$$q_x(x,y) = \frac{1}{\pi(3+\nu)} \int_{-\infty}^{\infty} \hat{f}(\xi)\, \mathrm{e}^{-|\xi|x-\mathrm{i}\xi y}\, \mathrm{d}\xi, \tag{26}$$

$$q_y(x,y) = \frac{\mathrm{i}}{\pi(3+\nu)} \int_{-\infty}^{\infty} \frac{\hat{f}(\xi)}{|\xi|}\, \xi\, \mathrm{e}^{-|\xi|x-\mathrm{i}\xi y}\, \mathrm{d}\xi, \tag{27}$$

$$v_x(x,y) = \frac{1}{2\pi(3+\nu)} \int_{-\infty}^{\infty} \hat{f}(\xi)((3+\nu)+(1-\nu)|\xi|x)\, \mathrm{e}^{-|\xi|x-\mathrm{i}\xi y}\, \mathrm{d}\xi \tag{28}$$

and

$$v_y(x,y) = \frac{-\mathrm{i}(1-\nu)}{2\pi(3+\nu)} \int_{-\infty}^{\infty} \frac{\hat{f}(\xi)}{|\xi|}\, \xi(-2+|\xi|x)\, \mathrm{e}^{-|\xi|x-\mathrm{i}\xi y}\, \mathrm{d}\xi. \tag{29}$$

Since the function $f(y)$ describing the prescribed equivalent shear force v_x can be divided into two parts, say, even part $f_1(y)$ and odd part $f_2(y)$, eqns (22)–(29) can be separated into two succinct groups as follows:

(a) for even function $f_1(y)$

$$w(x,y) = \frac{-1}{\pi(3+\nu)(1-\nu)D} \int_0^{\infty} \frac{\hat{f}_1(\xi)}{\xi^3} (2+(1-\nu)\xi x)\, \mathrm{e}^{-\xi x} \cos(\xi y)\, \mathrm{d}\xi, \tag{30}$$

$$m_x(x,y) = \frac{(1-\nu)x}{\pi(3+\nu)} \int_0^{\infty} \hat{f}_1(\xi)\, \mathrm{e}^{-\xi x} \cos(\xi y)\, \mathrm{d}\xi, \tag{31}$$

$$m_y(x,y) = \frac{-1}{\pi(3+\nu)} \int_0^{\infty} \frac{\hat{f}_1(\xi)}{\xi} (2(1+\nu)+(1-\nu)\xi x)\, \mathrm{e}^{-\xi x} \cos(\xi y)\, \mathrm{d}\xi, \tag{32}$$

$$m_{xy}(x,y) = \frac{1}{\pi(3+\nu)} \int_0^{\infty} \frac{\hat{f}_1(\xi)}{\xi} ((1+\nu)+(1-\nu)\xi x)\, \mathrm{e}^{-\xi x} \sin(\xi y)\, \mathrm{d}\xi, \tag{33}$$

$$q_x(x,y) = \frac{2}{\pi(3+\nu)} \int_0^{\infty} \hat{f}_1(\xi)\, \mathrm{e}^{-\xi x} \cos(\xi y)\, \mathrm{d}\xi, \tag{34}$$

$$q_y(x,y) = \frac{2}{\pi(3+\nu)} \int_0^{\infty} \hat{f}_1(\xi)\, \mathrm{e}^{-\xi x} \sin(\xi y)\, \mathrm{d}\xi, \tag{35}$$

$$v_x(x,y) = \frac{1}{\pi(3+\nu)} \int_0^{\infty} \hat{f}_1(\xi)((3+\nu)+(1-\nu)\xi x)\, \mathrm{e}^{-\xi x} \cos(\xi y)\, \mathrm{d}\xi \tag{36}$$

and

$$v_y(x,y) = \frac{-(1-\nu)}{\pi(3+\nu)}\int_0^\infty \hat{f}_1(\xi)(-2+\xi x)\,e^{-\xi x}\sin(\xi y)\,d\xi; \tag{37}$$

(b) for odd function $f_2(y)$

$$w(x,y) = \frac{-1}{\pi(3+\nu)(1-\nu)D}\int_0^\infty \frac{\hat{f}_2(\xi)}{\xi^3}(2+(1-\nu)\xi x)\,e^{-\xi x}\sin(\xi y)\,d\xi, \tag{38}$$

$$m_x(x,y) = \frac{(1-\nu)x}{\pi(3+\nu)}\int_0^\infty \hat{f}_2(\xi)\,e^{-\xi x}\sin(\xi y)\,d\xi, \tag{39}$$

$$m_y(x,y) = \frac{-1}{\pi(3+\nu)}\int_0^\infty \frac{\hat{f}_2(\xi)}{\xi}(2(1+\nu)+(1-\nu)\xi x)\,e^{-\xi x}\sin(\xi y)\,d\xi, \tag{40}$$

$$m_{xy}(x,y) = \frac{-1}{\pi(3+\nu)}\int_0^\infty \frac{\hat{f}_2(\xi)}{\xi}((1+\nu)+(1-\nu)\xi x)\,e^{-\xi x}\cos(\xi y)\,d\xi, \tag{41}$$

$$q_x(x,y) = \frac{2}{\pi(3+\nu)}\int_0^\infty \hat{f}_2(\xi)\,e^{-\xi x}\sin(\xi y)\,d\xi, \tag{42}$$

$$q_y(x,y) = \frac{-2}{\pi(3+\nu)}\int_0^\infty \hat{f}_2(\xi)\,e^{-\xi x}\cos(\xi y)\,d\xi, \tag{43}$$

$$v_x(x,y) = \frac{1}{\pi(3+\nu)}\int_0^\infty \hat{f}_2(\xi)((3+\nu)+(1-\nu)\xi x)\,e^{-\xi x}\sin(\xi y)\,d\xi \tag{44}$$

and

$$v_y(x,y) = \frac{(1-\nu)}{\pi(3+\nu)}\int_0^\infty \hat{f}_2(\xi)(-2+\xi x)\,e^{-\xi x}\cos(\xi y)\,d\xi. \tag{45}$$

In the above, the functions $\hat{f}_1(\xi)$ and $\hat{f}_2(\xi)$ are defined as:

$$\hat{f}_1(\xi) = 2\int_0^\infty f_1(y)\cos(\xi y)\,dy$$

and

$$\hat{f}_2(\xi) = 2\int_0^\infty f_2(y)\sin(\xi y)\,dy.$$

As seen in Fig. 1(c), consider an infinite thin plate with a crack of length $2a$ located at $x = 0$ and $|y| \leqslant a$. The crack surfaces are subjected to an arbitrary anti-symmetric equivalent shear force $v_x = f(y)$, which can be represented by a polynomial of order N. Hence, the boundary conditions are found as:

(1) $v_x = f(y) = -\sum_{n=0}^{N} C_n\left(\frac{y}{a}\right)^n$ at $x = 0,\ |y| \leqslant a$,

(2) $w = 0$ at $x = 0,\ |y| \geqslant a$,

(3) $m_x = 0$ at $x = 0$

and

(4) $w \to 0$ as $x \to \pm\infty$.

Due to the anti-symmetry of the equivalent shear force v_x, only the region $x \geqslant 0$ needs to be analysed. The above boundary conditions (3) and (4) are the same as the boundary conditions (ii) and (iii) of the problem as displayed in Fig. 2. Hence, eqns (30)–(45) are also applicable here. However, the determination of functions $\hat{f}_1(\xi)$ and $\hat{f}_2(\xi)$ needs to be derived from the boundary conditions (1) and (2). Furthermore, since the equivalent shear force v_x is represented by a polynomial as shown in condition (1), the complete analytical solution can be similarly expressed as the combination of the even and odd part solutions $f_1(y)$ and $f_2(y)$, respectively.

(a) For even order n

Let

$$f_1(y) = -\sum_{n=0,2,\ldots}^{N} C_n\left(\frac{y}{a}\right)^n.$$

Upon substituting the boundary conditions (1) and (2) into eqns (36) and (30) respectively, a pair of dual integral equations used to determine the function $\hat{f}_1(\xi)$ results in:

$$\left.\begin{aligned} &\frac{1}{\pi}\int_0^\infty \hat{f}_1(\xi)\cos(\xi y)\,\mathrm{d}\xi = f_1(y) \quad && a \geqslant y \geqslant 0 \\ &\int_0^\infty \hat{f}_1(\xi)\cos(\xi y)\frac{\mathrm{d}\xi}{\xi^3} = 0 \quad && y \geqslant a \end{aligned}\right\}. \tag{46}$$

Defining the following parameters:

$$\rho = a\xi,$$

$$\eta = \frac{y}{a},$$

$$g_1(\eta) = a\left(\frac{\pi}{2\eta}\right)^{1/2} f_1(y),$$

$$F_1(\rho) = \tfrac{1}{2}\rho^{-1/2}\hat{f}_1(\xi)$$

and

$$\cos(\rho\eta) = \left(\frac{\pi\rho\eta}{2}\right)^{1/2} J_{-1/2}(\rho\eta),$$

where J_r denotes the Bessel function of the first kind with order r (here $r = -\frac{1}{2}$), eqn (46) can be written as:

$$\left.\begin{aligned} &\int_0^\infty \rho^3 F_1(\rho) J_{-1/2}(\rho\eta)\,\mathrm{d}\rho = g_1(\eta) \quad && 1 \geqslant \eta \geqslant 0 \\ &\int_0^\infty F_1(\rho) J_{-1/2}(\rho\eta)\,\mathrm{d}\rho = 0 \quad && \eta \geqslant 1 \end{aligned}\right\}.$$

The solution of $F_1(\rho)$ can be obtained from Sneddon (1951) as:

$$F_1(\rho) = \left(\frac{2}{\pi\rho}\right)^{1/2} \int_0^1 y^{5/2} J_1(y\rho)\left(\int_0^1 g_1(yu)u^{1/2}(1-u^2)^{1/2}\,du\right)dy.$$

Hence, from the definition as stated above, one obtains:

$$\hat{f}_1(\xi) = -\tfrac{1}{2}a^3\pi^{1/2}\xi^2 \sum_{n=0,2,\ldots}^{N} \frac{\Gamma\left(\dfrac{n}{2}+\dfrac{1}{2}\right)}{\Gamma\left(\dfrac{n}{2}+2\right)} C_n \int_0^1 y^{n+2} J_1(a\xi y)\,dy, \tag{47}$$

where $\Gamma(\cdot)$ represents the Gamma function. Substituting eqn (47) into eqns (30)–(37), the analytical solutions for w, m_x, m_y, m_{xy}, q_x, q_y, v_x and v_y, due to equivalent shear force with even order n are thus found in terms of the coefficients C_n.

(b) For odd order n

Similarly, let

$$f_2(y) = -\sum_{n=1,3,\ldots}^{N} C_n\left(\frac{y}{a}\right)^n.$$

To substitute the boundary condition (1) and (2) into eqns (44) and (38) respectively, a pair of dual integral equations used to determine the function $\hat{f}_2(\xi)$ is obtained as:

$$\left.\begin{aligned} \frac{1}{\pi}\int_0^\infty \hat{f}_2(\xi)\sin(\xi y)\,d\xi &= f_2(y) \quad a \geqslant y \geqslant 0 \\ \int_0^\infty \hat{f}_2(\xi)\sin(\xi y)\frac{d\xi}{\xi^3} &= 0 \qquad y \geqslant a \end{aligned}\right\}. \tag{48}$$

Defining the functions $g_2(\eta)$, $\hat{f}_2(\xi)$ and $\sin(\rho\eta)$ as follows:

$$g_2(\eta) = a\left(\frac{\pi}{2\eta}\right)^{1/2} f_2(y),$$

$$F_2(\rho) = \tfrac{1}{2}\rho^{-1/2}\hat{f}_2(\xi)$$

and

$$\sin(\rho\eta) = \left(\frac{\pi\rho\eta}{2}\right)^{1/2} J_{1/2}(\rho\eta).$$

Equation (48) can be rewritten as:

$$\left.\begin{aligned} \int_0^\infty \rho^3 F_2(\rho) J_{1/2}(\rho\eta)\,d\rho &= g_2(\eta) \quad 1 \geqslant \eta \geqslant 0 \\ \int_0^\infty F_2(\rho) J_{1/2}(\rho\eta)\,d\rho &= 0 \qquad \eta \geqslant 1 \end{aligned}\right\}.$$

From Sneddon (1951), $F_2(\rho)$ is defined as:

$$F_2(\rho) = \left(\frac{2}{\pi\rho}\right)^{1/2} \int_0^1 y^{5/2} J_2(y\rho) \int_0^1 g_2(yu) u^{3/2} (1-u^2)^{1/2} \, du \, dy,$$

and $\hat{f}_2(\xi)$ is thus given by:

$$\hat{f}_2(\xi) = -\tfrac{1}{2} a^3 \pi^{1/2} \xi^2 \sum_{n=1,3,\ldots}^{N} \frac{\Gamma\left(\frac{n}{2}+1\right)}{\Gamma\left(\frac{n}{2}+\frac{5}{2}\right)} C_n \int_0^1 y^{n+2} J_2(a\xi y) \, dy. \tag{49}$$

Again, substituting eqn (49) into eqns (38)–(45), the analytical solutions for w, m_x, m_y, m_{xy}, q_x, q_y, v_x and v_y due to equivalent shear force with odd order n can thus be obtained in terms of the coefficients C_n.

3. CALCULATION OF BENDING/SHEAR STRESS INTENSITY FACTORS

For a cracked plate in bending, the fracture behavior is usually described by the bending and shear stress intensity factors as defined by Sih *et al.* (1962). From the relation between stresses (σ_{xx}, τ_{xy}) and moments (m_x, m_{xy}) in plate theory (Szilard, 1974), K_b and K_s can be expressed as

$$K_b = \lim_{y \to a} \frac{6}{h^2} \sqrt{2(y-a)}\, m_x(0, y)$$

and

$$K_s = \lim_{y \to a} \frac{(3+\nu)}{(1+\nu)} \frac{6}{h^2} \sqrt{2(y-a)}\, m_{xy}(0, y).$$

As stated earlier, the analytical solution and bending stress intensity factor for the problem subjected to arbitrary symmetric bending moment as shown in Fig. 1(b) have been solved (Chen *et al.*, 1992). Attention is thus focused on solving the shear stress intensity factor K_s. Substituting the aforementioned analytical solution of m_{xy} into the above expression, after tedious manipulations, the shear stress intensity factor K_s can be obtained as:

$$K_s = \sum_{n=0,2,\ldots}^{N} \frac{3}{h^2} C_n a\sqrt{a} \frac{n!}{2^n[(n/2)!]^2(n+2)/2} + \sum_{n=1,3,\ldots}^{N} \frac{3}{h^2} C_n a\sqrt{a} \frac{(n+1)!}{2^{n+1}\{[(n+1)/2]!\}^2(n+3)/2}. \tag{50}$$

For completeness, the analytical solution of bending stress intensity factor for the problem as shown in Fig. 1(b) is quoted below (Chen *et al.*, 1992):

$$K_b = \sum_{n=0,2,\ldots}^{N} \frac{6}{h^2} C_n^* \sqrt{a} \frac{n!}{2^n[(n/2)!]^2} + \sum_{n=1,3,\ldots}^{N} \frac{6}{h^2} C_n^* \sqrt{a} \frac{(n+1)!}{2^{n+1}\{[(n+1)/2]!\}^2}, \tag{51}$$

where C_n^* $(n = 0, 1, 2, \ldots)$ are the coefficients of the polynomial used for fitting the bending moment applied on crack surfaces. The analytical solutions for w, m_x, m_y, m_{xy}, q_x, q_y, v_x and v_y due to bending moment can also be expressed in terms of the coefficients C_n^* $(n = 0, 1, 2, \ldots)$.

As seen in Fig. 1, based on the principle of superposition, the complete analytical solution for w, m_x, m_y, m_{xy}, q_x, q_y, v_x, v_y, K_b and K_s due to bending moment and equivalent shear force can be expressed in terms of the coefficients C_n^* and C_n ($n = 0, 1, 2, \ldots$) in matrix form as:

$$\{Q\} = [T]\{C\} \tag{52}$$

and

$$\{K\} = [S]\{C\}, \tag{53}$$

where the column vectors $\{Q\}$, $\{K\}$ and $\{C\}$ are defined as:

$$\{Q\} = \lfloor w, m_x, m_y, m_{xy}, q_x, q_y, v_x, v_y \rfloor^{\mathrm{T}},$$
$$\{K\} = \lfloor K_{bA}, K_{bB}, K_{sA}, K_{sB} \rfloor^{\mathrm{T}}$$

and

$$\{C\} = \lfloor C_0^*, C_1^*, \ldots, C_N^*, C_0, C_1, \ldots, C_N \rfloor^{\mathrm{T}}.$$

$[T]$, $[S]$ are the matrix of the relation function between the analytical solution vectors ($\{Q\}$, $\{K\}$) and the coefficient vector $\{C\}$ for $(w, m_x, m_y, m_{xy}, q_x, q_y, v_x, v_y)$ and (K_b, K_s). Both $[T]$ and $[S]$ are functions of crack length. In addition, $[T]$ is also a function of space. As a result, once the coefficient vector $\{C\}$ is determined, the vector $\{Q\}$ at any location of the plate and the stress intensity factors $\{K\}$ can be calculated from eqns (52) and (53). The details of the finite element alternating procedure, such as how the coefficient vector $\{C\}$ is determined from the conventional finite element solution of the uncracked geometry, and how the method is achieved in a finite element formulation can be referred to Chen *et al.* (1922) and, for want of space, are not repeated here.

4. TREATMENT OF CONSTANT TWISTING MOMENTS ON THE CRACK SURFACES

In the finite element alternating procedure (Chen *et al.*, 1992; Chen and Chang, 1989a, b, 1990), the residual stresses at the location of fictitious cracks need to be obtained and released. In fact, the residual stresses for thin plates in bending contain bending, twisting moment and transverse shear force. But those three types of loadings cannot all be applied to the crack surfaces directly. Kirchhoff assumptions show that the equivalent shear force can be expressed in terms of the derivative of twisting moment and transverse shear force (Szilard, 1974). Hence, the constant twisting moment behaves as trivial in the computation of the equivalent shear force. Therefore, suitable treatment of the constant twisting moment is essential to compute accurate mixed mode (bending/shear) stress intensity factors.

Without loss of generality, consider an infinite plate containing a crack of length $2a$ subjected to a constant twisting moment per unit crack length $m_{xy} = -m_0 (m_0 > 0)$ on the crack surfaces (see Fig. 3). The shear stress intensity factor can be derived from Sih (1973a) as:

$$K_s = \frac{6}{h^2} m_0 \sqrt{a}, \tag{54}$$

h is the thickness of the thin plate. To simulate the twisting effect, an odd polynomial should be selected for describing the equivalent shear force v_x^*. Hence, to give a good approximation, the equivalent shear force v_x^* which has the same twisting effect of the constant twisting moment ($-m_0$) is assumed as:

$$v_x^* = -C_1\left(\frac{y}{a}\right) - C_3\left(\frac{y}{a}\right)^3. \tag{55}$$

As a result of the constant twisting moment, one has

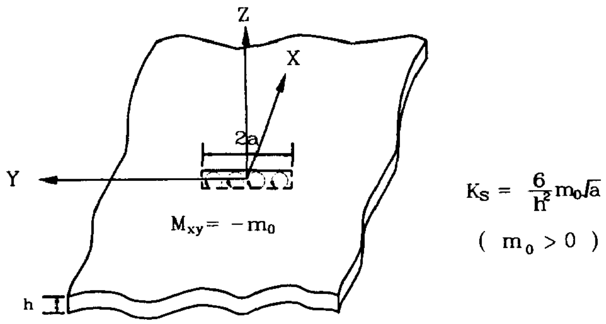

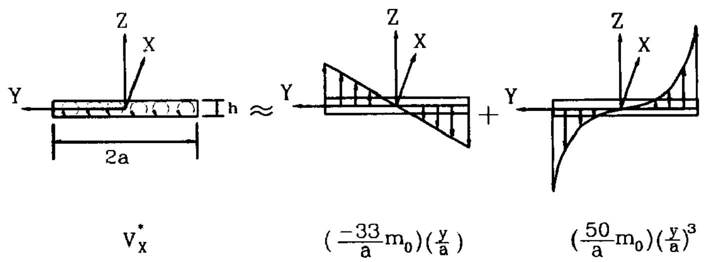

Fig. 3. Treatment of constant twisting moment on crack surfaces.

$$2a(-m_0) = \int_{-a}^{a} (-C_1)\left(\frac{y}{a}\right) y \, dy + \int_{-a}^{a} (-C_3)\left(\frac{y}{a}\right)^3 y \, dy. \tag{56}$$

In addition, due to the nature of the twisting moment, only the odd part of the shear stress intensity factor is created. Hence, from eqns (50) and (54), one reaches

$$K_s = \frac{6}{h^2} m_0 \sqrt{a} \sim \sum_{n=1,3}^{3} \frac{3}{h^2} C_n a \sqrt{a} \frac{(n+1)!}{2^{n+1}\{[(n+1)/2]!\}^2 (n+3)/2}. \tag{57}$$

From the relations (56) and (57), C_1 and C_3 can be determined and the equivalent shear force v_x^* of eqn (55) can be expressed as:

$$v_x^* = \left(\frac{-33}{a} m_0\right)\left(\frac{y}{a}\right) + \left(\frac{50}{a} m_0\right)\left(\frac{y}{a}\right)^3. \tag{58}$$

Thus, once a constant twisting moment $(-m_0)$ on the crack surfaces of a thin plate is encountered, the modified equivalent shear force v_x^* of eqn (58) should be taken into account.

5. RESULTS AND DISCUSSIONS

To verify the validity and efficiency of the method proposed, several plate problems in bending with single or two cracks are analysed. The computation can be performed to analyse the cases with more cracks without any difficulty. The interaction effect between the cracks on the computation of bending/shear stress intensity factors is also studied. As for finite element modeling, the simple four-node plate element (each node has four degrees of freedom w, $w_{,x}$, $w_{,y}$ and $w_{,xy}$) is employed in all analyses. The Poisson's ratio used in the problems analysed is 0.3.

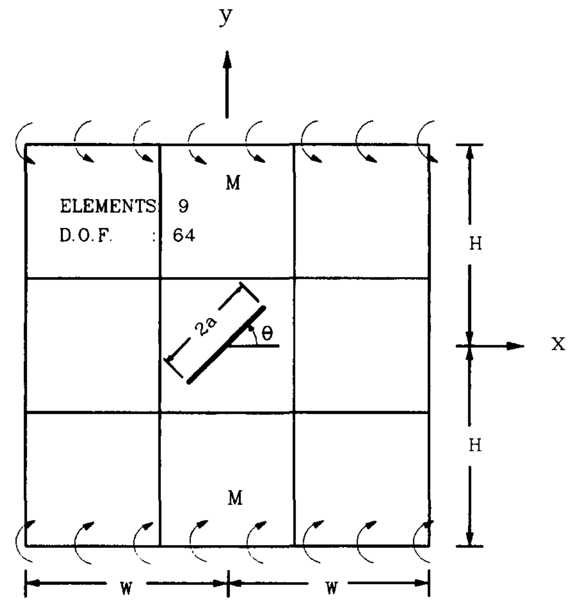

Fig. 4. Finite element mesh for a plate containing an inclined crack.

Example 1. A square plate with a central crack subjected to uniform bending

As seen in Figs 4 and 5, a square plate containing a mixed mode crack subjected to uniform bending along the boundary at $y = \pm H$ is first solved. The geometry and its finite element mesh with nine elements are also shown. The variation of the present computed stress intensity factors K_b and K_s normalized by the value of $3M\sqrt{a}/h^2$ versus various inclined angles is displayed in Fig. 5 for the case of $a/W = 1/15$. For the purpose of comparison the analytical normalized stress intensity factors (Sih *et al.*, 1962) for an infinite plate are also shown. Excellent results show the high accuracy of the present finite element alternating procedure.

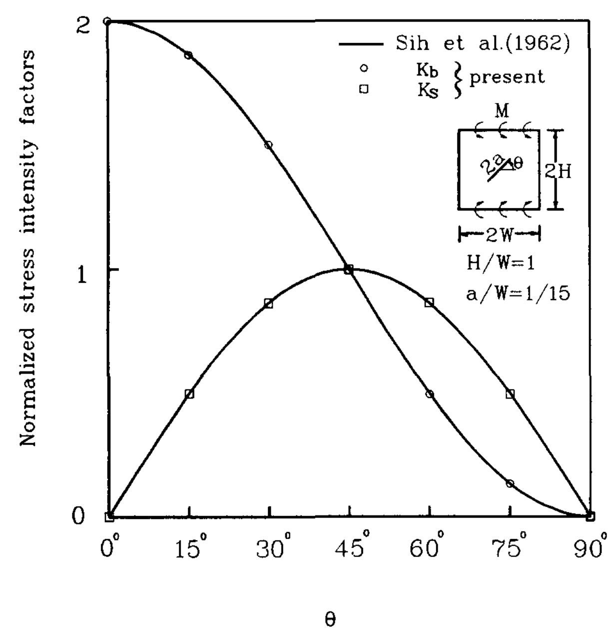

Fig. 5. Variation of normalized stress intensity factors versus inclined angles θ.

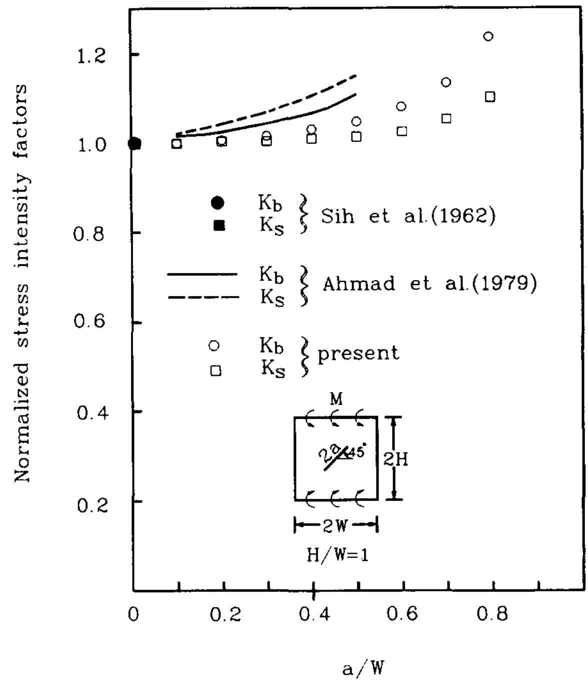

Fig. 6. Variation of normalized stress intensity factors versus crack length ratios.

The variation of the normalized stress intensity factors K_b and K_s versus various crack lengths is displayed in Fig. 6 for the case of $\theta = 45°$. The results obtained by Ahmad and Loo (1979) using a specialized finite element technique near the crack-tip are also shown. As displayed in Ahmad and Loo (1979), higher results are obtained as a more coarser mesh is adopted. Hence, if a more finer mesh is used, it is expected that the solutions of Ahmad and Loo (1979) should converge to the present solutions. It is noted that the present computed bending stress intensity factor K_b is always greater than the shear stress intensity factor K_s except for the cases with small cracks (as the crack is small, as seen in Fig. 5, the bending stress intensity factor K_b should be identical to the shear stress intensity factor K_s). Such a phenomenon is also observed in the cases of two-dimensional fracture problems (Chen and Chang, 1989a) and all other cases presented in this work.

The order N of the polynomials taken for fitting the bending moment and equivalent shear force on crack surfaces is four. Higher order polynomials advance the results slightly. Since the solution converges very fast, the number of iteration is never greater than three. However, when the crack is close to the plate boundary, the residual stress near the boundary becomes more complex and more elements (or more iterations) need to be included. For each iteration, the CPU time consumed is about the same as the conventional finite element calculation for the uncracked plate using the same simple mesh.

Example 2. A rectangular plate with two inclined cracks subjected to uniform bending

To examine the interaction effect among multiple cracks, for simplicity, a rectangular plate containing two inclined cracks which are symmetric to the y-axis and subjected to uniform bending at $y = \pm H$ is solved here. The geometry and finite element mesh can be seen in Fig. 7. Figures 8 and 9 display the variations of normalized bending and shear stress intensity factors versus various inclined angles, respectively. Also shown is the analytical solution for the infinite plate obtained by the present alternating procedure (Chen *et al.*, 1992; Chen and Chang, 1990) only. As would be expected, the stress intensity factors of the bounded plate are always larger than those of the infinite plate. In addition, the stress intensity factors of crack-tip B are always larger than those of crack-tip A due to the interaction effect among cracks. Besides, as seen in Fig. 8, such an interaction effect for

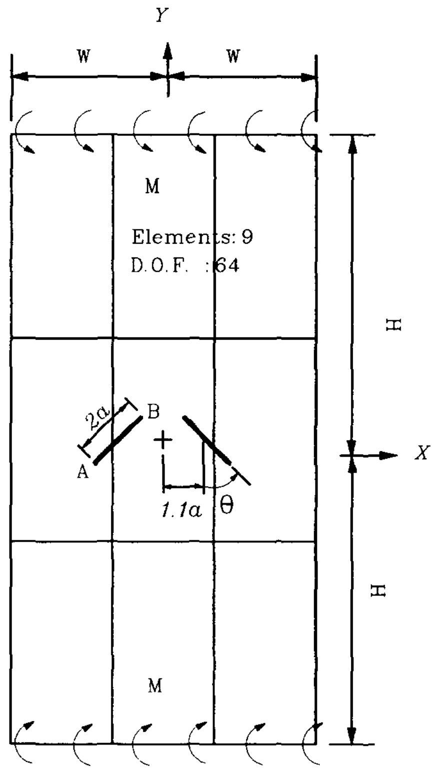

Fig. 7. Finite element mesh for a rectangular plate with two inclined cracks ($H/W = 2$, $a/W = 0.25$).

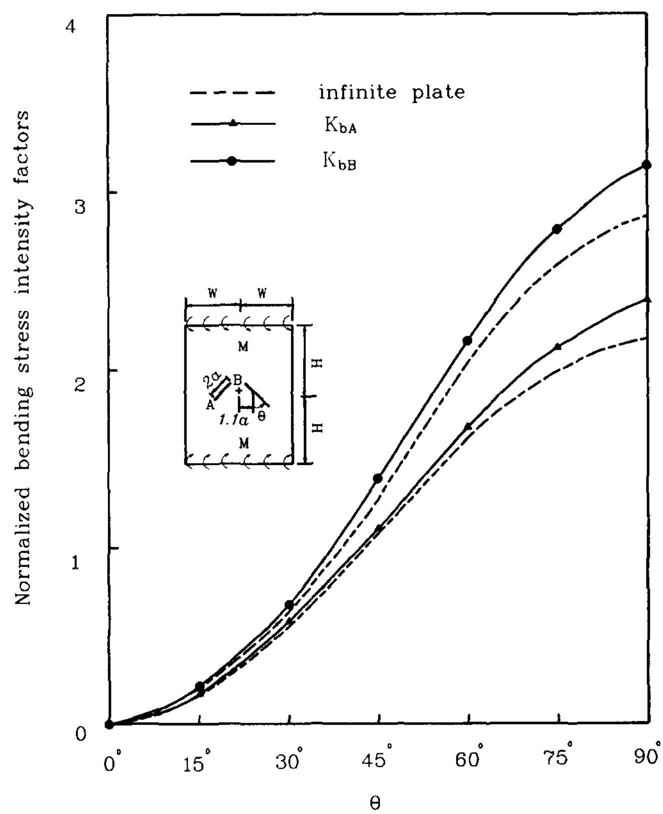

Fig. 8. Normalized bending stress intensity factors for the rectangular plate with two inclined cracks.

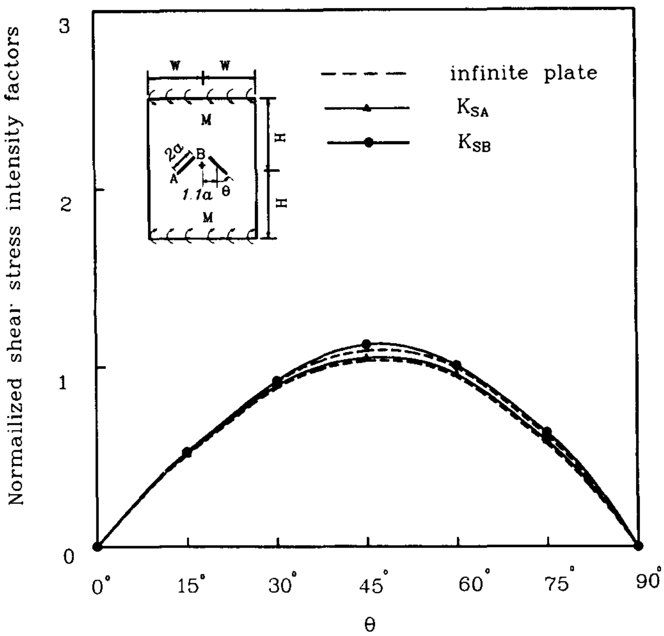

Fig. 9. Normalized shear stress intensity factors for the rectangular plate with two inclined cracks.

bending stress intensity factors increases with the inclined angles. For shear stress intensity factors, however, the interaction effect reaches its maxima at $\theta = 45°$ (see Fig. 9).

6. CONCLUSIONS

The analytical solution for an infinite plate with a crack subjected to arbitrary anti-symmetric shear force on crack surfaces has been successfully derived. Suitable treatment of constant twisting moment on crack surfaces is made. Based on these, an efficient and accurate finite element alternating procedure is thus developed to analyse the plate problems in bending with single or multiple mixed mode cracks. To evaluate the bending/shear stress intensity factors accurately, only a very limited number of regular elements are required and the computer cost is much more economical as compared with those needed by conventional finite element calculations, especially for the problem with multiple cracks.

This work can be further extended to deal with thick or moderately thick cracked plates in bending.

REFERENCES

Ahmad, J. and Loo, F. T. C. (1979). Solution of plate bending problems in fracture mechanics using a specialized finite element technique. *Engng Fract. Mech.* **11**, 661–673.

Babuška, I. and Oh, H. S. (1990). The p-version of the finite element method for domains with corners and for infinite domains. *Numer. Meth. PDEs* **6**, 371–392.

Barsoum, R. S. (1976). A degenerate solid element for linear fracture analysis of plate bending and general shells. *Int. J. Numer. Meth. Engng* **10**, 551–564.

Chen, W. H. and Chang, C. S. (1989a). Analysis of two dimensional mixed mode crack problems by finite element alternating method. *Comput. Struct.* **33**(6), 1451–1458.

Chen, W. H. and Chang, C. S. (1989b). Analysis of two dimensional fracture problems with multiple cracks under mixed boundary condition. *Engng Fract. Mech.* **34**(4), 921–934.

Chen, W. H. and Chang, C. S. (1990). Analysis of multiple cracks in an infinite plate under arbitrary surface tractions. *Ing. Archiv.* **60**, 202–212.

Chen, W. H. and Chen, P. Y. (1984). A hybrid-displacement finite element model for the bending analysis of thin cracked plates. *Int. J. Fract.* **24**, 83–106.

Chen, W. H., Yang, K. C. and Chang, C. S. (1992). A finite element alternating approach for the bending analysis of thin cracked plates. *Int. J. Fract.* **56**(2), 93–110.

Jirousek, J. (1985). Implementation of local effects into conventional and non-conventional finite element formulations. In *Local Effects in the Analysis of Structures* (Edited by P. Ladeveze), pp. 279–298. Elsevier, Amsterdam.

Jirousek, J. and Guex, L. (1986). The Hybrid–Trefftz finite element model and its application to plate bending. *Int. J. Numer. Meth. Engng* **23**, 651–693.

Jirousek, J. and Venkatesh, A. (1990). A new FE approach for adaptive reliability assurance. *Comput. Struct.* **37**(2), 217–230.

Murthy, M. V. V., Raju, K. N. and Viswanath, S. (1981). On the bending stress distribution at the tip of a stationary crack from Reissner's theory. *Int. J. Fract.* **17**, 537–552.

Rhee, H. C. and Atluri, S. N. (1982). Hybrid stress finite element analysis of bending of a plate with a through flaw. *Int. J. Numer. Meth. Engng* **18**, 259–271.

Sih, G. C. (1973a). *Handbook of Stress Intensity Factors for Research Engineers.* Lehigh University Press, New York.

Sih, G. C. (1973b). Methods of Analysis and Solutions of Crack Problems. *Mechanics of Fracture I.* Noordhoff, Leyden, The Netherlands.

Sih, G. C., Paris, P. C. and Erdogan, F. (1962). Crack-tip stress intensity factors for plane extension and plate bending problems. *ASME J. Appl. Mech.* **29**, 306–312.

Sneddon, I. N. (1951). *Fourier Transforms.* McGraw-Hill, New York.

Szilard, R. (1974). *Theory and Analysis of Plates: Classical and Numerical Methods.* Prentice-Hall, New Jersey.

Williams, M. L. (1961). The bending stress distribution at the base of a stationary crack. *ASME J. Appl. Mech.* **28**, 78–82.

Yagawa, G. and Nishioka, T. (1979). Finite element analysis of stress intensity fracture factors for plane extension and plate bending problems. *Int. J. Numer. Meth. Engng* **14**, 727–740.

Ye, T. Q. and Gallagher, R. H. (1984). A singular finite element for analysis of plate bending problem in fracture mechanics. *Int. J. Fract.* **24**, 137–147.